A Ductile - Fracture Instability Model Based upon Production of Geometrically - Necessary Dislocations

W. W. Gerberich and W. Reuter

Of late, increasing evidence points towards deformation about second phase particles as being the controlling mechanism in the ductile fracture of high strength materials. The present study was an attempt to correlate the dislocation dynamics of a tensile bar to the discontinuous crack propagation in a fracture toughness test.

Experimental Techniques and Results

An acoustic emission technique[1] recorded the low amplitude dislocation events associated with plastic flow in tensile specimens. In another set of tests, a stress-wave emission device[2] recorded large-amplitude cracking events in 6-inch wide center-cracked plates. The material was ½-inch thick 7075 aluminum aged to four conditions.

From engineering and true stress-strain plots, the data for the first four columns of Table 1 were obtained. The acoustic emission data were found to be described by

$$\dot{N} = m_p' \varepsilon_p e^{-\phi \varepsilon_p} \qquad (1)$$

where $\dot{N}$ is the number of counts per second; m_p' and ϕ are constants; and ε_p is the true plastic strain. Such a plot is shown in Fig. 1 for the peak-aged condition. Since $d\dot{N}/d\varepsilon_p = 0$ in Eq. (1) gives $\varepsilon_p = 1/\phi$, ϕ is obtained directly from the peak of the $\dot{N}$ - ε_p plot and m_p' is adjusted to give the best fit to the downward slope of the curve.

From eight large plate fracture tests, 12 sets of data were obtained representing fracture instabilities. About half of these were large shear instabilities in the as-quenched samples which could be directly measured. These were associated with stress intensity levels ranging from 66,400 to 102,500 psi-in$^{\frac{1}{2}}$. From the other conditions, measures of the average length of crack jump, ℓ_{OBS}, were determined from the macroscopic growth increment divided by the number of stress waves, N_{SWE}, occurring in the increment. These were associated with stress intensity levels ranging from 37,000 to 75,000 psi-in$^{\frac{1}{2}}$. The results, as given in terms of the average ℓ_{OBS} for each condition correlated with both n and ϕ, the result for ϕ being shown in Fig. 2.

Table 1. FLOW PARAMETERS FOR 7075 ALUMINUM ALLOY

CONDITION	σ_{ys} 1000 psi	σ_{ULT} 1000 psi	n	ϕ	$10^5 m_p'$ $10^{11}/cm^2$	$2f/br$ $10^{11}/cm^2$
As Quenched	22.1 22.5	58.9 57.6	0.213 0.231	1820 940	258 208	140 140
Aged 250°F 4 hr.	62.0 59.8	76.7 83.5	0.080 0.087	50.5 —	0.58 —	— —
Aged T6	73.0 72.0	83.5 83.3	0.064 0.057	81.3 81.3	0.77 1.55	2.8 2.8
T6 + Aged 350°F, 12 hr.	56.1 57.2	69.3 70.2	0.072 0.070	102 —	1.95 —	— —

+ For as-quenched: $b = 2.96$ Å; $f \simeq 0.05$; $r \simeq 25$ Å for G.P. zones
For T6: $b = 2.86$ Å; center-to-center spacing of 2000 Å; $r = 500$ Å; $f \simeq 0.02$. Based upon E-phase ($Cr_2Mg_3Al_{18}$) on fracture surface.

Theoretical Interpretations

First, what does the acoustic emission data represent? One may consider two classes of interpretations, one where $\dot{N}$ represents mobile dislocation density and one where it represents rate of occurrence of dislocation events. For the first class, one might consider dislocation dynamics in the Gilman sense[3] or for precipitation-hardening systems, Ashby's[4] work-hardening model. If one considers ρ_{mD} as being the number of mobile dislocations being detected by the transducer, then one can show that as the dislocation spacing decreases, at some point ρ_{mD} would decrease. Interpreting this in terms of Ashby's model and invoking an effective particle radius, then $r_{eff} = r\exp(\phi\varepsilon_p)$ and a modified Ashby model would give

$$\rho_{mD} \approx \frac{2f}{br}\varepsilon_p^{-\phi\varepsilon_p} \qquad (2)$$

One might note that this is identical to the Gilman model with ϕ being a work-hardening parameter and $2f/br$ being the breeding factor as given in terms of volume fraction, f, particle radius, r, and Burgers vector, b. Each acoustic emission count rate pulse has been suggested[5] to be made up of $10^5 - 10^6$ breakaway dislocation events. In a similar vein, one can use $10^5 m_p'$ to give the right order of magnitude breeding factor. If one does this in Table 1 and independently calculates $2f/br$ where the parameters are approximately known, one finds a reasonable comparison between the last two columns in Table 1.

For the second class, one can interpret $\dot{N}$ as the rate of dislocation breakaway[5] or, in the present case, the rate of production of geometrically necessary dislocations. Physically, $d\rho^G/d\varepsilon_p$ could decrease to some small value when particle decohesion, shear or fracture started. Keeping the same functional form as above, then

$$\frac{d\rho^G}{d\varepsilon_p} = \frac{\alpha 2f}{br}\varepsilon_p e^{-\phi\varepsilon_p} \qquad (3)$$

where α is some constant on the order of 10^3 to 10^4. If one integrates Eq. (3), then a continuously increasing value of ρ^G with strain is found. In any event, considering the recent literature[2,5], one may conclude that one of these approaches represents the likely source for the acoustic emission. At this point it is of value to consider possible fracture models.

Krafft[6] suggested that fracture proceeded in a process zone, d_T, close to the crack tip when the strain reached a critical value, ε_{CR}. For a plane strain situation where Poisson's ratio is 0.3, using the conditions $\sigma_y, \sigma_x = \sigma_y$ and $\sigma_z = 2\nu\sigma_y$ leads to

$$K = \varepsilon_{CR} E[8\pi d_T]^{\frac{1}{2}} \qquad (4)$$

where K is the applied stress intensity and E is Young's modulus. Krafft suggested that ε_{CR} is the strain associated with a macroscopic tensile instability. However, the stress-strain relationship is also a function of dislocation density. Thus, if one considers local plastic instability between particles, then one could use the criterion that $d\rho_{mD}/d\varepsilon_p = 0$. From Eq. (2) this occurs at $\varepsilon_{CR} = 1/\phi$ so that the Krafft criterion becomes

$$d_T = \frac{1}{8\pi}\left(\frac{K\phi}{E}\right)^2 . \qquad (5)$$

For the high stress intensity levels where conditions are not plane strain, Eq. (5) is about two orders of magnitude too high. However, if one considers just the relatively plane strain cases, then for $K \sim 40{,}000$ psi-in$^{\frac{1}{2}}$ and $\phi \sim 80$, d_T is calculated to be 0.004 in. while the observed values ranged from 0.001 to 0.004 in.

For the second model, a strain distribution based upon the tensile analogy of the elastic-plastic Mode III situation is used to define the total region in the vicinity of the particle where the fracture strain is exceeded. In this case, the condition for fracture could be that

the rate of production of geometrically-necessary dislocations drops to some low value as described above. As a first approximation, let $d\rho^G/d\varepsilon_p \rightarrow \alpha \varepsilon_p$, and take the log of Eq. (3) which gives $\varepsilon_p = \ln(2f/br)\phi^{-1}$. If, as the final event of microvoid coalescence, this strain is that leading to fracture, the insertion into the strain distribution gives a fractured region, ℓ^*, of

$$\ell^* = \frac{\phi K^2}{3\pi\sigma_{ys} E \ln(2f/br)} \qquad (6)$$

It might be pointed out that even if the estimate of $d\rho^G/d\varepsilon_p$ is off by several orders of magnitude, this only makes a factor of two difference in the estimate of ℓ^*. Using the observed values of ϕ, K, σ_{ys}, E and the value of $10^5\ m_p'$ for $2f/br$, the theoretical fit of Eq. (6) to the observed crack jumps is seen in Fig. (3).

In summary, it can be said that both fracture models give the right trend to the data with the latter being more accurate. However, absolute magnitudes mean relatively little here because of the approximate nature of several of the assumptions. Since ϕ is also a function of the particle characteristics, it is not possible to further differentiate between these two approaches without additional study.

REFERENCES AND ACKNOWLEDGEMENTS

1. R. G. Liptai, D. O. Harris, R. B. Engle and C. A. Tatro, Int. J. Non-destructive Test., 3, (1971) p. 215.
2. C. E. Hartbower, W. W. Gerberich and H. Liebowitz, J. Eng. Fract. Mech., 1, (1968), p. 291.
3. J. J. Gilman, Proc. 5th U.S. Nat. Cong. Appl. Mech., ASTM New York (1966), p. 385.
4. M. F. Ashby, Phil. Mag., 21, (1970), p. 399.
5. D. R. James and S. H. Carpenter, J. Appl. Phys., 42, 12, November (1971), p. 4685.
6. J. M. Krafft, App. Mat'ls. Res., 3, (1963), p. 88.

7. ACKNOWLEDGEMENTS: The authors are deeply indebted to H. Dunnegan, formerly at Lawrence Radiation Laboratory in Livermore, for much of the acoustic emission data. This work was supported by the Atomic Energy Commission and the Office of Naval Research.

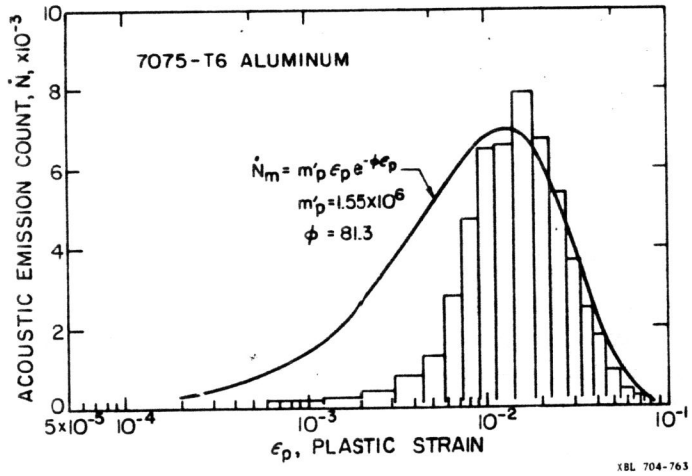

Fig. 1: Acoustic Emission Count Rate From Tensile Test.

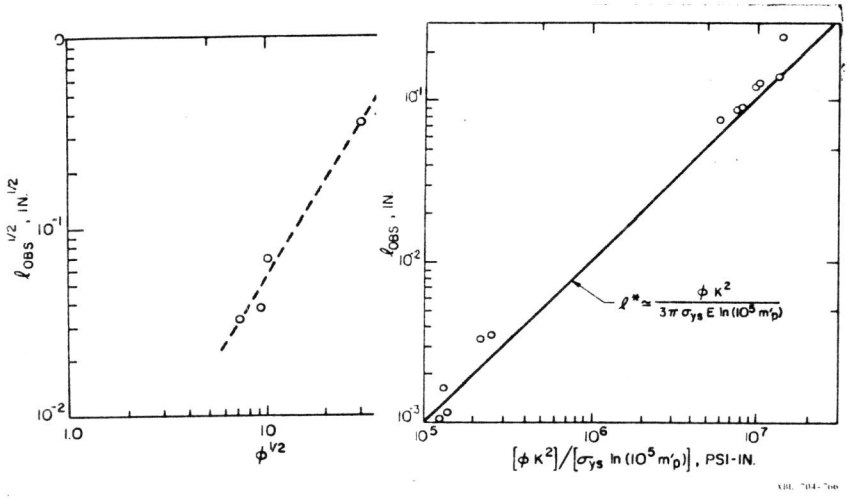

Fig. 2: Crack Jumps Versus Dislocation Parameter From Tensile Tests.

Fig. 3: Actual Crack Jumps Compare To Calculations From Fracture Model.